Data Repository Appendix 1. Site setting and methods

Site setting

Lago Teo (LT) is located in the immediate vicinity of the Chaitén Township, ~8 km SSW from Volcán Chaitén (VC) (Data Repository Figure 1), and provides a detailed record of pyroclastic fallout deposits by virtue of its relatively high-sediment accumulating rates and constant depositional environment in an enclosed-basin lake isolated from, and perched well above the Río Chaitén floodplain. The lake is elliptical shape, has a maximum length of 185 meters, a surface area of ~2 ha and a single concave depression with a maximum water depth of 5 meters. Here we obtained two overlapping sediment cores from an anchored raft equipped with a 10-cm wide aluminum casing, using a 5-cm diameter Wright piston corer and a sediment-water interface piston corer with a 7.5-cm diameter Plexiglas chamber. The stratigraphy of the cores was characterized by lithological descriptions, digital X-radiographs (Data Repository Figure 2), and loss-on-ignition analysis following overnight drying at 105°C. We performed sequential burns at 550°C and 925°C for 2 and 4 hours, respectively, to quantify the organic, carbonate, and siliciclastic content of the sediments (Bengtsson and Enell, 1986; Heiri et al., 2001).

The geomorphologic setting, distance and location of LT relative to VC allows this lake to record most explosive eruptions from VC avoiding the deposition of fluvio-laharic detritus as well as thick and/or coarse-grained tephra carried predominantly eastward by the prevailing westerly winds. The small catchment area of LT and absence of inlet streams into the basin maximizes a local sedimentary record of predominantly or exclusively airfall

tephras, ruling out advection of reworked tephras into the site by fluvial or slope processes. A high-resolution palynological record developed from the LT core demonstrates continuous cover of Valdivian/North Patagonian rainforests and absence of major lake-level changes in the site which, along with the predominance of organic-rich lake mud, demonstrate depositional and environmental constancy in the basin.

Chronology

The chronology of the LT record is constrained by 23 AMS radiocarbon dates (Data Repository Table 1) obtained from 1-cm thick sections along the core which, along with a core top age of -61 yr BP for the sediment-water interface, afford the basis for a Bayesian age model (Data Repository Figure 3) using the Bacon (Blaauw and Christen, 2011) package for R. This model takes into account the instantaneous deposition of all tephras by subtracting their cumulative thickness throughout the core. The tephra-free age model of LT suggests uninterrupted lacustrine sedimentation with relatively constant accumulation rate of lake sediments (median: 19.6 cm/kyr over the last ~10,000 years) (Data Repository Figure 3). We note that the tephra from the 2008 Chaitén eruption (LTT-1) occurs between depths 6-9 cm (Figure 1, Data Repository Table 2) suggesting that this dense layer penetrated the uncompressed, partially suspended sediment-water interface on the lake floor. For this reason we decided not to carry out ^{210}Pb measurements on the upper portion of the water-sediment interface core. Our modeled age of 200 yr BP for LTT-1 must be taken with caution considering that this tephra occurs in the high-sediment accumulation, water-saturated uncompressed zone of the sediment core, and it constitutes an interpolation

between the core top age -61 yr BP and the age of AMS date UCIAMS-126075 (median probability calibrated age of 394 yr BP, Data Repository Table 2). We interpret the modeled age of LTT-1 as an upper age limit for the effects of tephra penetration into previously deposited soft organic lake sediments, a factor that probably affects the interpolated and actual ages associated to all tephras in the LT record and, most likely, similar sites throughout our study area.

Geochemistry

All major element determinations were made on a JEOL Superprobe ± JXA-8230 housed at Victoria University of Wellington, using the ZAF correction method. Analyses were performed using an accelerating voltage of 15 kV under a static electron beam operating at 8 nA. The electron beam was defocused between 10 and 20 μm. Oxide values are recalculated to 100% on a volatile-free basis. Total Fe expressed as FeO_t. We were unable to analyze some tephras ± LTT-11, LTT-13, LTT-16, LTT-19, LTT-21, LTT-24, either because of their fine grain-size (silicic) or the prevalence and density of crystal microlites within the glass matrix (andesitic to basaltic).

References

Bengtsson, L., and Enell, M., 1986, Chemical analysis, *in* Berglund, B.E., ed., Handbook of Palaeoecology and Palaeohydrology, John Wiley & Sons, p. 423-451.

Blaauw, M., and Christen, J.A., 2011, Flexible Paleoclimate Age-Depth Models Using an Autoregressive Gamma Process: Bayesian Analysis, v. 6, p. 457-474.

Heiri, O., Lotter, A.F., and Lemcke, G., 2001, Loss on ignition as a method for estimating organic and carbonate content in sediments: reproducibility and comparability of results: Journal of Paleolimnology, v. 25, p. 101-110.

Data Repository Figure 1. Map of southern South America and the study area showing the location of Lago Teo, Chaiten township and nearly volcanic centres. Also indicated are selected andic cover-bed sections where proximal Volcan Chaiten (VC) and Michimahuida Volcanic Complex (MVC) tephra sequences have been described and sampled for comparative glass geochemistry (see Figure 2).

Data Repository Figure 2. X-radiographs of sediment cores obtained from Lago Teo. Core 0301BT1 is shown in the left followed by cores 0301AT1, 0301AT2 and 0301AT3 from left to right. Individual core tops oriented toward the top.

Data Repository Figure 3. Probability distribution of individual calibrated radiocarbon-age measurements from Lago Teo (blue pattern), also shown is the Bayesian age applied to the calendar age data. The intensity of the gray pattern represents the probability density of the age models bounded by dashed lines that represent the 95% confidence limits.

Data Repository Figure 4. CaO and K2O vs FeOt and K2O vs SiO2 (wt %) contents of glass shards from rhyolitic tephra layers preserved in the Lago Teo core. Analyses from the 2008 Chaitén eruption are included for comparison (Alloway & Villarosa, *this study*).

Data Repository Figure 5. Tephrostratigraphy of the Lago Teo sediment core compared with equivalent-aged andic cover-bed sections in the same vicinity containing both Volcán

Chaitén (VC) and Michinmahuida Volcanic Complex (MVC)-sourced tephra beds. See Figure 1 for site locations and Figure 3 for geochemical composition of MVC and rhyolitic tephras.

Data Repository Table 1. Tephra codes (LTT= Lago Teo Tephra), depth ranges and interpolated calibrated ages for each pyroclastic layer in the Lago Teo record. Yellow highlighted samples are rhyolitic tephras from VC, green highlighted samples are from MVC. We calculate time steps of 397 ± 325 yr between pyroclastic layers from all sources over the past ~10,000 yr and 227 ± 186 yr between VC events over the last millennium (mean ± 1σ), considering the correct calendar age for LTT-1 in both cases.

Data Repository Table 2. Information on the radiocarbon dates from the Lago Teo record. All radiocarbon dates were converted to calendar ages before present using the southern hemisphere calibration dataset included in the CALIB 6.0 software.

Data Repository Table 3. Summary of glass shard major element compositions of tephra beds preserved in Lago Teo. Mean ± 1 standard deviation, based on *n* analyses. All samples are normalized against glass standards ATHO-G & VG-568. [1]Chaitén samples (*unpublished data* retrieved from 17 proximal & distal localities collected by G. Villarosa, V. Outes and B.V. Alloway). Compositional Groups: 1 – rhyolite (R), 2 – trachyte (T), dacite (D); 3 – basaltic trachyandesite (BTA), trachyandesite (TA), basaltic andesite (BA),

andesite (A) (see Figure 2). Compositional fields after Le Maitre (1984). Analyst: B.V. Alloway.

Data Repository Table 4. Glass-shard electron microprobe data from the 2008 Chaitén eruption compared with silicic tephra preserved in Lago Teo. [1]Samples retrieved from 17 proximal and distal localities.

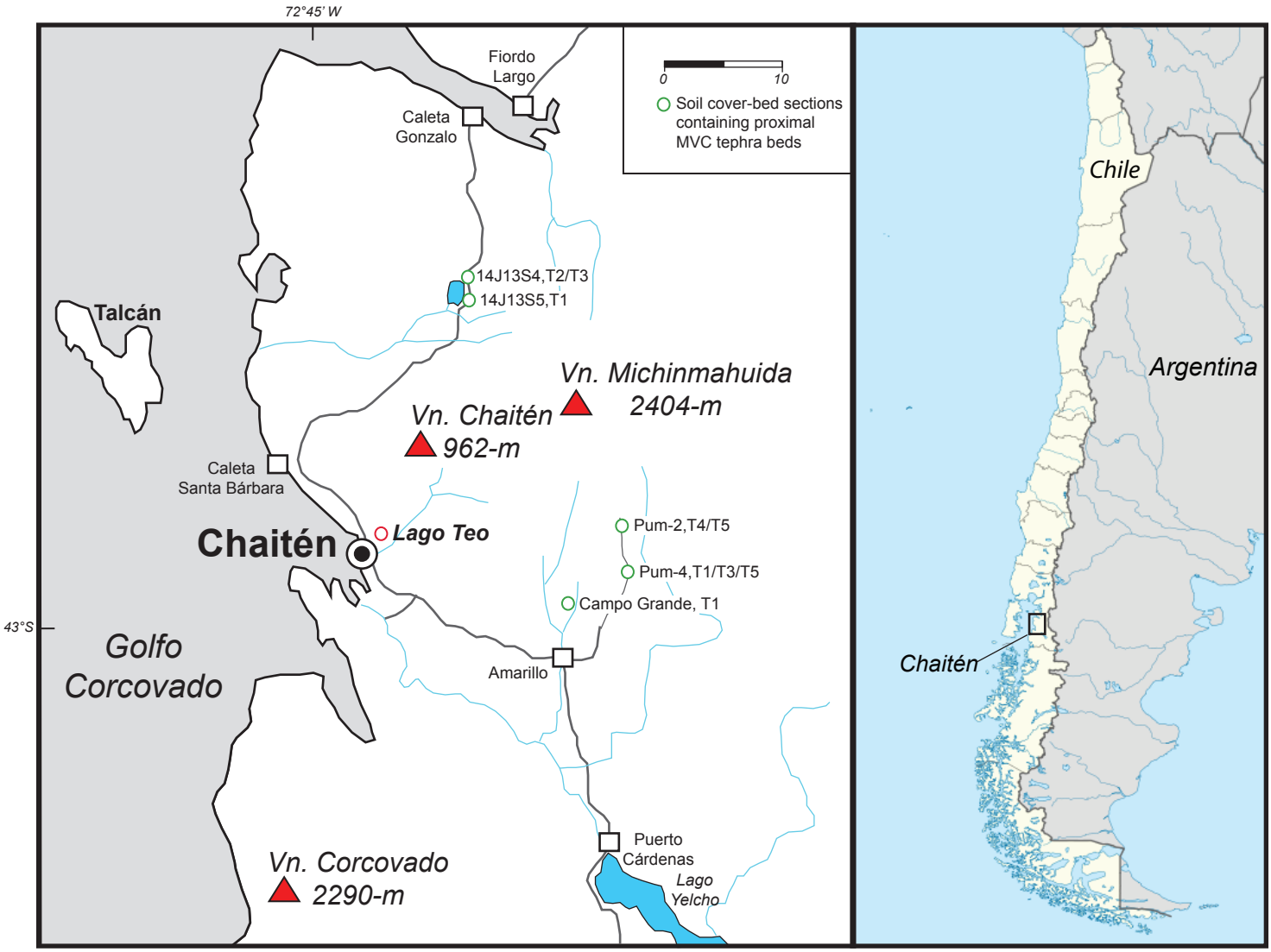
72°45' W
43°S
Fiordo
Largo
Caleta
Gonzalo
0
10
Soil cover-bed sections
containing proximal
MVC tephra beds
14J13S4,T2/T3
14J13S5,T1
Talcán
Vn. Michinmahuida
2404-m
Vn. Chaitén
962-m
Caleta
Santa Bárbara
Chaitén
Lago Teo
Pum-2,T4/T5
Pum-4,T1/T3/T5
Campo Grande, T1
Amarillo
Golfo
Corcovado
Vn. Corcovado
2290-m
Puerto
Cárdenas
Lago
Yelcho
Chile
Argentina
Chaitén

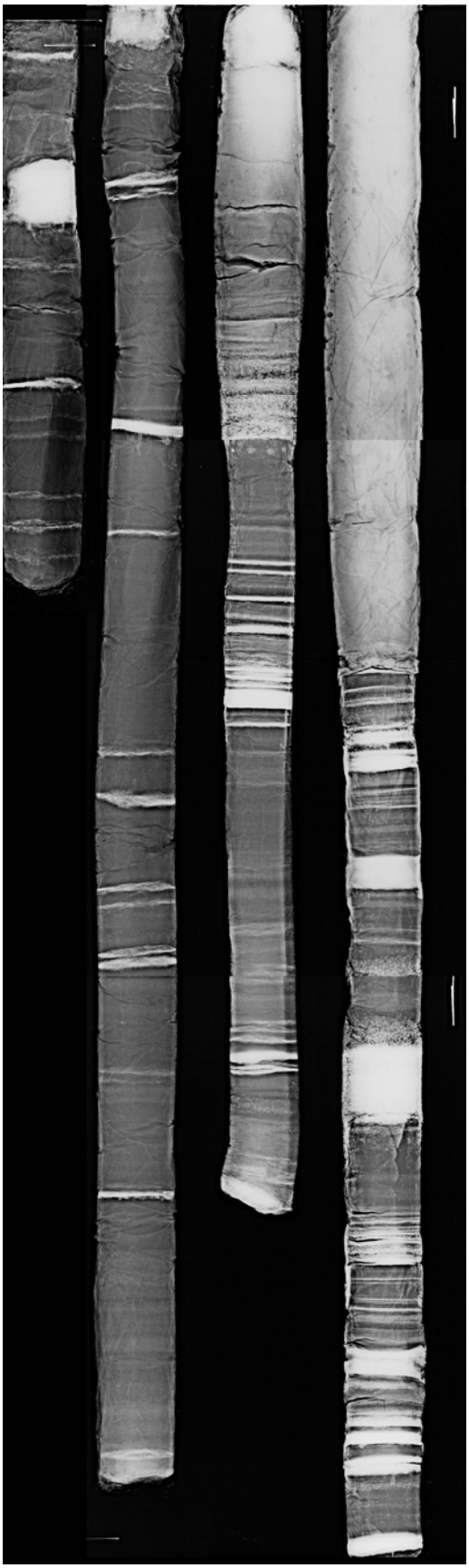

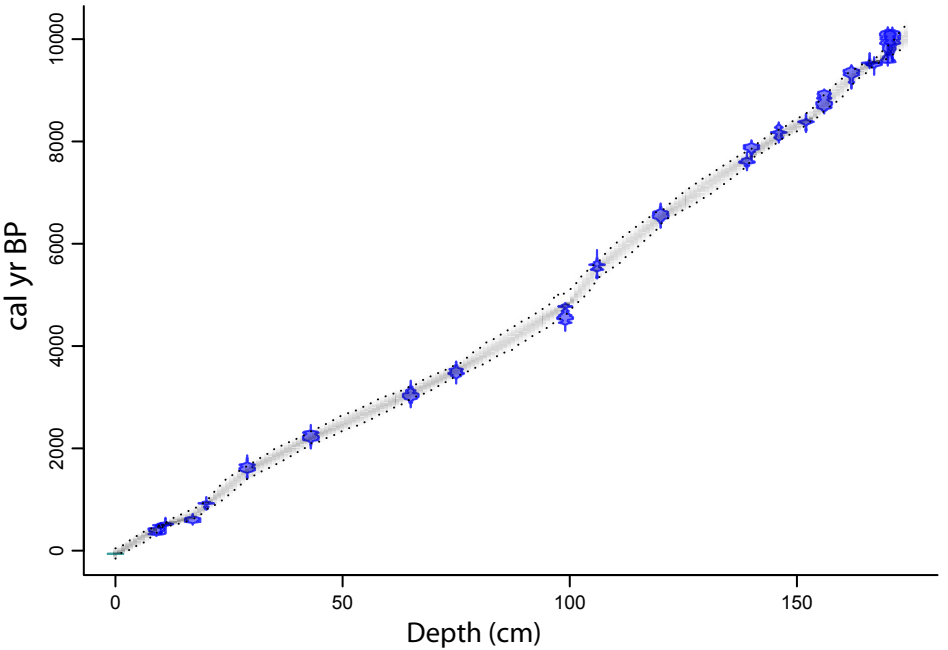
cal yr BP
0
2000
4000
6000
8000
10000
0
50
100
150
Depth (cm)

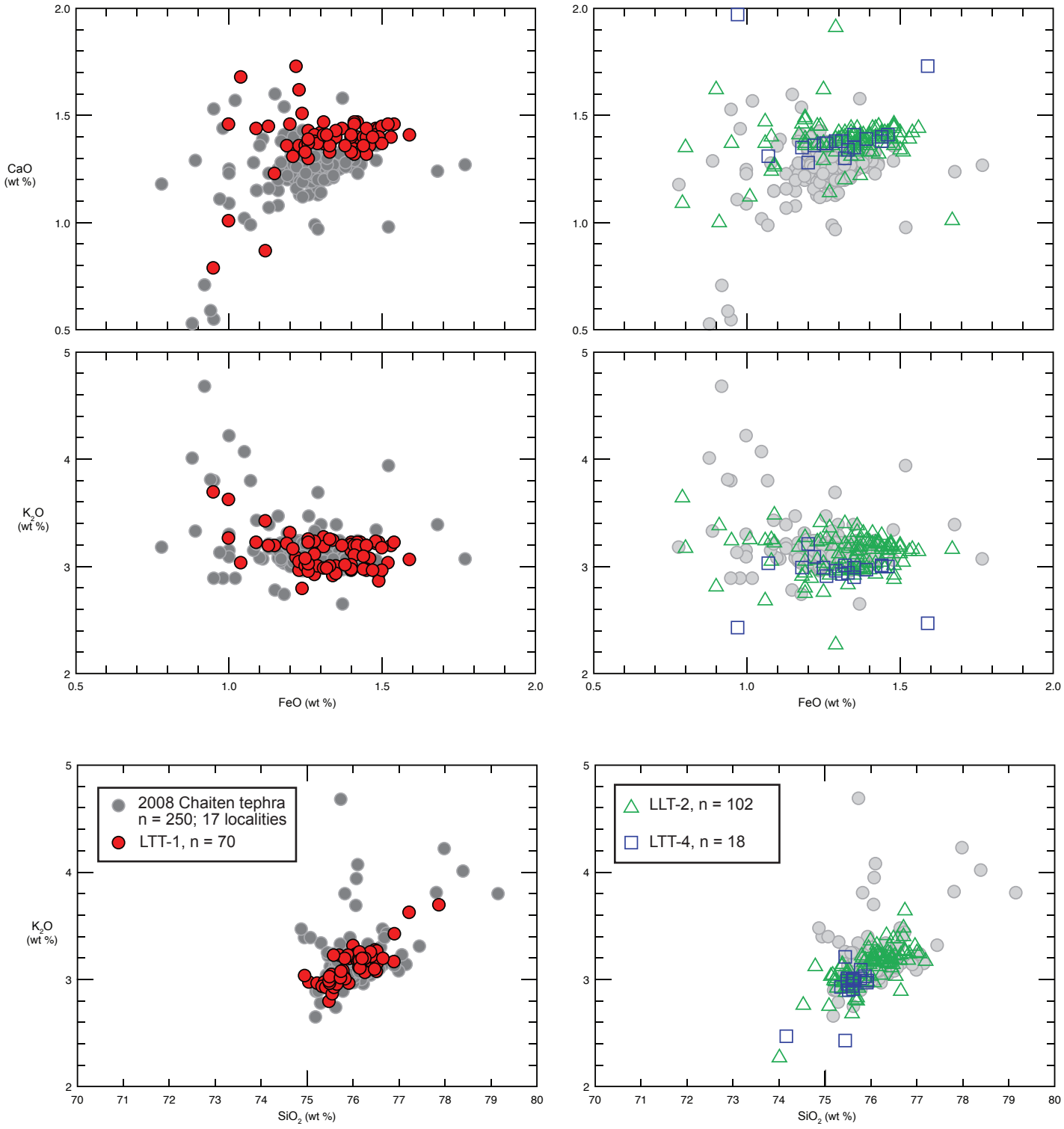
CaO (wt %)
K2O (wt %)
FeO (wt %)
2008 Chaiten tephra
n = 250; 17 localities
LTT-1, n = 70
LLT-2, n = 102
LTT-4, n = 18
SiO2 (wt %)

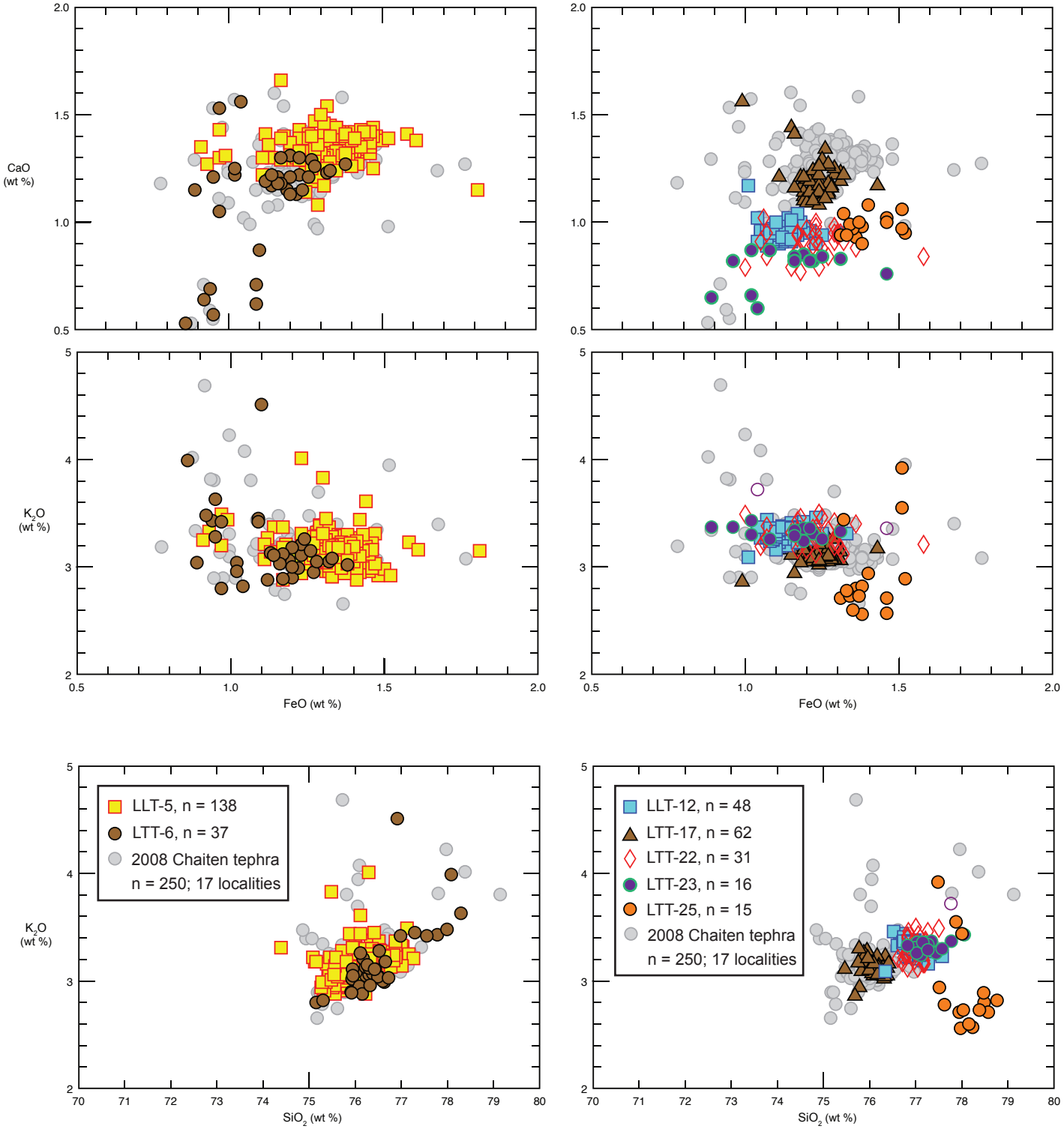
CaO (wt %)
K2O (wt %)
FeO (wt %)
FeO (wt %)
K2O (wt %)
SiO2 (wt %)
SiO2 (wt %)
LLT-5, n = 138
LTT-6, n = 37
2008 Chaiten tephra
n = 250; 17 localities
LLT-12, n = 48
LTT-17, n = 62
LTT-22, n = 31
LTT-23, n = 16
LTT-25, n = 15
2008 Chaiten tephra
n = 250; 17 localities

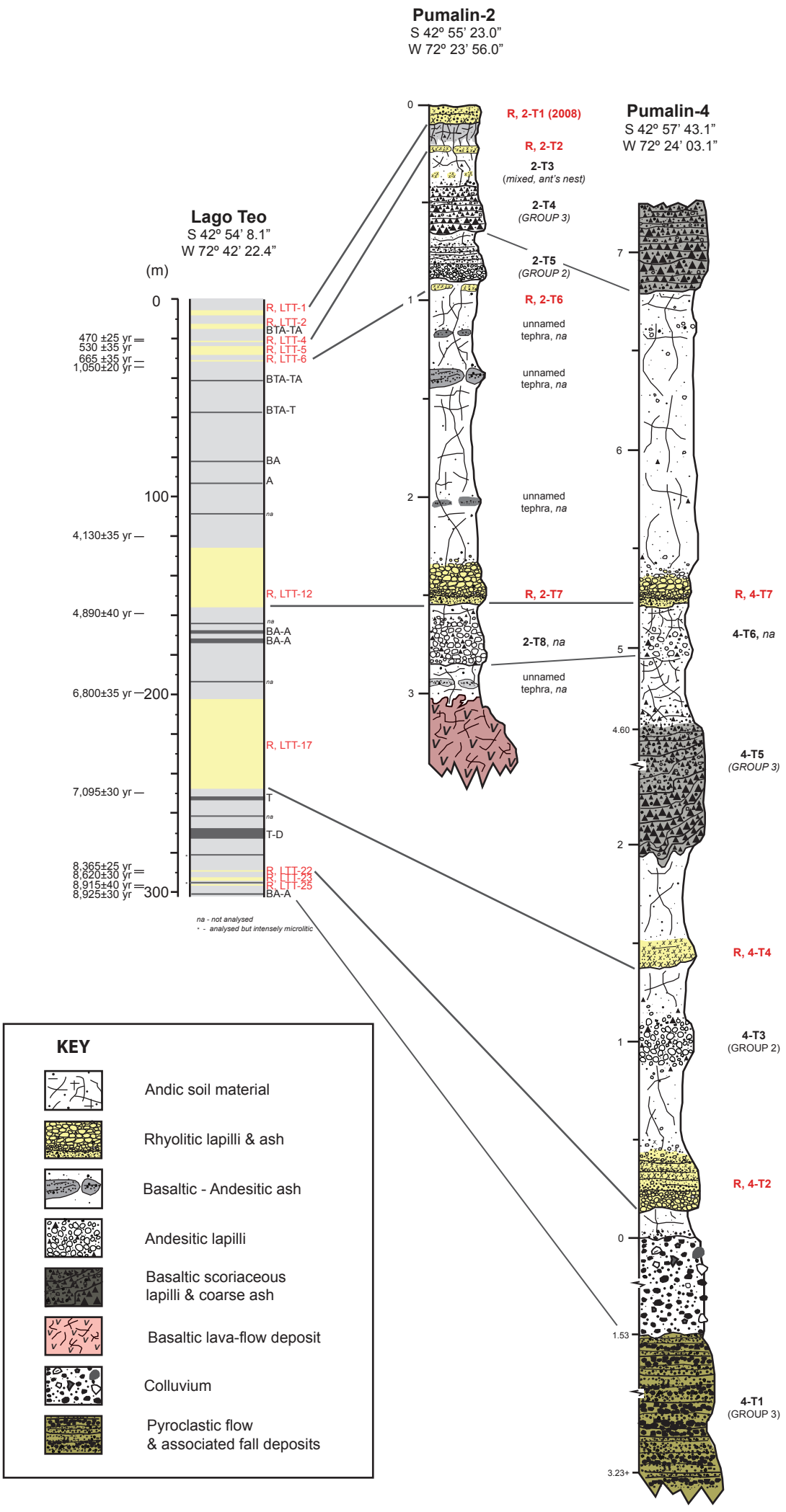
Pumalin-2
S 42º 55' 23.0"
W 72º 23' 56.0"
Pumalin-4
S 42º 57' 43.1"
W 72º 24' 03.1"
Lago Teo
S 42º 54' 8.1"
W 72º 42' 22.4"
(m)
0
100
200
300
470 ±25 yr
530 ±35 yr
665 ±35 yr
1,050±20 yr
4,130±35 yr
4,890±40 yr
6,800±35 yr
7,095±30 yr
8,365±25 yr
8,620±30 yr
8,915±40 yr
8,925±30 yr
R, LTT-1
R, LTT-2
BTA-TA
R, LTT-4
R, LTT-5
R, LTT-6
BTA-TA
BTA-T
BA
A
na
R, LTT-12
na
BA-A
BA-A
na
R, LTT-17
T
na
T-D
R, LTT-22
R, LTT-23
R, LTT-25
BA-A
na - not analysed
* - analysed but intensely microlitic
R, 2-T1 (2008)
R, 2-T2
2-T3
(mixed, ant's nest)
2-T4
(GROUP 3)
2-T5
(GROUP 2)
R, 2-T6
unnamed tephra, na
unnamed tephra, na
unnamed tephra, na
R, 2-T7
2-T8, na
unnamed tephra, na
0
1
2
3
7
6
5
4.60
2
1
0
1.53
3.23+
R, 4-T7
4-T6, na
4-T5
(GROUP 3)
R, 4-T4
4-T3
(GROUP 2)
R, 4-T2
4-T1
(GROUP 3)
KEY
Andic soil material
Rhyolitic lapilli & ash
Basaltic - Andesitic ash
Andesitic lapilli
Basaltic scoriaceous lapilli & coarse ash
Basaltic lava-flow deposit
Colluvium
Pyroclastic flow & associated fall deposits

phra code	Depth range (cm)	Thickness (cm)	Interpolated age Median (cal yr BP)	Interpolated age ±2σ (cal yr BP)
LTT-1	6-9	3	200	117-332
LTT-2	13-15	2	416	343-485
LTT-3	15-16	1	471	404-508
LTT-4	22-23	1	598	561-751
LTT-5	24-29	5	629	591-794
LTT-6	32-33	1	851	755-943
LTT-7	41-43	2	1554	1281-1599
LTT-8	57-59	2	2194	2002-2284
LTT-9	82-84	2	2980	2939-3200
LTT-10	93-95	2	3508	3338-3593
LTT-11	108-110	2	4028	3919-4339
LTT-12	126-157	31	5078	4906-5364
LTT-13	165-166	1	5895	5587-6052
LTT-14	169-170	1	6059	5821-6266
LTT-15	172-175	3	6195	5984-6409
LTT-16	193-195	2	7360	7144-7533
LTT-17	201-249	48	7692	7569-7832
LTT-18	252-255	3	7901	7777-8044
LTT-19	261-263	2	8269	8132-8376
LTT-20	268-274	6	8488	8411-8664
LTT-21	281-283	2	9151	8946-9306
LTT-22	289-291	2	9462	9445-9603
LTT-23	293-294	1	9592	9543-9727
LTT-24	294-295	1	9617	9557-9757
LTT-25	296-297	1	9678	9594-9839
LTT-26	301-302	1	9861	9821-10,246

Laboratory code	Depth with tephras (cm)	Depth without tephras (cm)	^{14}C yr BP ±1σ	cal yr BP (-2σ)	cal yr BP (+2σ)	cal yr BP (median)
UCIAMS-126075	12-13	9-10	345±20	308	449	394
UCIAMS-126076	16-17	10-11	470±25	455	522	498
CAMS-141076	17-18	11-12	530±35	496	549	522
CAMS-141075	29-30	17-18	665±35	551	655	605
UCIAMS-126077	33-34	20-21	1050±20	818	960	925
CAMS-141077	44-45	29-30	1765±35	1537	1706	1617
CAMS-141078	60-61	43-44	2285±35	2151	2337	2233
UCIAMS-126078	84-85	65-66	2955±25	2929	3200	3036
CAMS-141079	96-97	75-76	3315±35	3387	3575	3483
CAMS-141080	122-123	99-100	4130±35	4435	4704	4572
CAMS-141036	160-161	106-107	4890±40	5470	5655	5562
CAMS-141037	179-180	120-121	5815±35	6452	6658	6559
UCIAMS-123011	200-201	139-140	6800±35	7518	7672	7606
UCIAMS-123002	249-250	140-141	7095±30	7792	7951	7881
CAMS-141038	258-259	146-147	7415±30	8038	8311	8176
UCIAMS-123003	266-267	152-153	7620±30	8325	8425	8382
CAMS-141039	276-277	156-157	7990±30	8635	8980	8777
UCIAMS-123004	284-285	162-163	8365±25	9143	9219	9342
UCIAMS-123005	288-289	166-167	8620±30	9480	9583	9534
UCIAMS-123006	291-292	167-168	8555±30	9466	9540	9506
CAMS-141487	297-298	170-171	8915±40	9744	10,171	9991
UCIAMS-123009	297-298	170-171	8705±30	9538	9685	9597
UCIAMS-123010	298-299	171-172	8925±30	9782	10,172	10,016

Tephra	SiO_2	Al_2O_3	TiO_2	FeO	MgO	MnO	CaO	Na_2O	K_2O	Cl	Total	*n*	Group
LTT-1	76.00 ± 0.51	14.02 ± 0.23	0.12 ± 0.03	1.34 ± 0.14	0.22 ± 0.04	0.02 ± 0.03	1.39 ± 0.13	3.74 ± 0.47	3.12 ± 0.16	0.09 ± 0.01	100.59 ± 0.66	70	1
LTT-2	75.99 ± 0.57	13.98 ± 0.18	0.12 ± 0.02	1.32 ± 0.16	0.21 ± 0.05	0.03 ± 0.03	1.38 ± 0.11	3.82 ± 0.56	3.11 ± 0.18	0.09 ± 0.01	100.66 ± 0.89	102	1
LTT-3	55.83 ± 0.37	14.20 ± 0.29	2.34 ± 0.09	11.15 ± 0.32	3.14 ± 0.11	0.09 ± 0.11	6.59 ± 0.12	4.83 ± 0.23	1.79 ± 0.12	0.10 ± 0.01	101.42 ± 0.61	30	3
LTT-4	75.54 ± 0.38	13.91 ± 0.15	0.13 ± 0.01	1.30 ± 0.14	0.26 ± 0.08	0.05 ± 0.02	1.42 ± 0.17	4.46 ± 0.29	2.93 ± 0.19	nd	100.26 ± 0.67	18	1
LTT-5	76.02 ± 0.52	13.95 ± 0.17	0.11 ± 0.03	1.33 ± 0.12	0.18 ± 0.09	0.08 ± 0.10	1.35 ± 0.08	3.79 ± 0.48	3.16 ± 0.17	0.09 ± 0.01	99.90 ± 1.99	138	1
LTT-6	76.50 ± 0.71	13.56 ± 0.41	0.10 ± 0.03	1.13 ± 0.13	0.18 ± 0.05	0.06 ± 0.02	1.13 ± 0.25	4.16 ± 0.28	3.14 ± 0.24	0.09 ± 0.01	99.95 ± 0.89	37	1
LTT-7	55.88 ± 0.53	13.97 ± 0.48	2.44 ± 0.16	11.71 ± 0.45	3.42 ± 0.35	0.23 ± 0.03	6.64 ± 0.44	3.82 ± 0.43	1.80 ± 0.30	0.09 ± 0.01	100.40 ± 0.71	33	3
LTT-8 Pop. 1	68.02 ± 0.46	16.11 ± 0.15	0.68 ± 0.04	3.52 ± 0.18	0.70 ± 0.08	0.13 ± 0.02	1.71 ± 0.17	5.79 ± 0.17	3.26 ± 0.12	0.17 ± 0.01	100.14 ± 1.12	12	2
Pop. 2	57.62 ± 2.71	16.70 ± 0.19	1.42 ± 0.15	7.69 ± 1.15	3.59 ± 0.86	0.15 ± 0.02	6.37 ± 1.32	4.73 ± 0.34	1.69 ± 0.41	0.10 ± 0.01	99.05 ± 0.67	21	3
LTT-9	54.99 ± 0.29	15.08 ± 0.21	1.95 ± 0.04	10.82 ± 0.23	4.62 ± 0.47	0.21 ± 0.02	7.10 ± 0.15	3.66 ± 0.14	1.56 ± 0.07	nd	98.31 ± 0.74	16	3
LTT-10	58.59 ± 0.63	15.70 ± 0.35	1.46 ± 0.05	8.45 ± 0.24	3.86 ± 0.26	0.16 ± 0.02	6.24 ± 0.28	4.02 ± 0.21	1.51 ± 0.09	nd	98.44 ± 0.78	15	3
LTT-12	76.10 ± 0.21	14.02 ± 0.12	0.11 ± 0.02	1.23 ± 0.06	0.25 ± 0.03	0.06 ± 0.02	1.20 ± 0.09	3.92 ± 0.10	3.12 ± 0.08	nd	97.17 ± 1.82	48	1
LTT-14	56.73 ± 0.55	16.09 ± 0.46	1.40 ± 0.08	9.36 ± 0.48	4.48 ± 0.31	0.18 ± 0.03	7.07 ± 0.34	3.61 ± 0.24	1.08 ± 0.06	nd	98.56 ± 0.67	13	3
LTT-15	57.06 ± 1.55	15.23 ± 0.99	1.95 ± 0.11	10.38 ± 0.58	3.64 ± 0.40	0.20 ± 0.02	6.25 ± 0.46	3.85 ± 0.31	1.45 ± 0.12	nd	99.05 ± 1.73	8	3
LTT-17	76.92 ± 0.21	13.60 ± 0.12	0.08 ± 0.01	1.13 ± 0.05	0.18 ± 0.02	0.06 ± 0.02	0.96 ± 0.04	3.77 ± 0.12	3.31 ± 0.07	nd	96.89 ± 2.57	62	1
LTT-18	65.74 ± 0.21	15.91 ± 0.12	0.91 ± 0.03	5.19 ± 0.19	0.97 ± 0.05	0.15 ± 0.03	2.34 ± 0.13	5.25 ± 0.18	3.52 ± 0.05	nd	98.86 ± 1.30	15	2
LTT-20	67.92 ± 0.86	16.13 ± 0.29	0.51 ± 0.06	3.81 ± 0.20	0.67 ± 0.09	0.12 ± 0.02	2.36 ± 0.20	5.14 ± 0.40	3.35 ± 0.35	nd	95.52 ± 4.47	30	2
LTT-21 *Contaminated (intensely microlitic)*	*58.77 ± 2.42*	*15.10 ± 1.72*	*1.40 ± 0.32*	*9.11 ± 1.76*	*3.71 ± 1.43*	*0.14 ± 0.05*	*6.51 ± 1.06*	*3.94 ± 0.60*	*1.26 ± 0.23*	*0.07 ± 0.02*	*99.11 ± 2.34*	*14*	*nd*
LTT-22	77.00 ± 0.22	13.30 ± 0.14	0.09 ± 0.01	1.22 ± 0.11	0.16 ± 0.04	0.07 ± 0.03	0.90 ± 0.06	3.92 ± 0.18	3.30 ± 0.11	0.08 ± 0.01	99.76 ± 1.28	31	1
LTT-23	77.29 ± 0.34	12.97 ± 0.16	0.08 ± 0.01	1.15 ± 0.14	0.11 ± 0.03	0.07 ± 0.02	0.80 ± 0.08	4.10 ± 0.13	3.35 ± 0.11	0.08 ± 0.01	101.67 ± 0.50	16	1
LTT-24 *Contaminated (intensely microlitic)*	*63.09 ± 2.94*	*15.61 ± 1.89*	*0.99 ± 0.43*	*6.51 ± 2.20*	*2.41 ± 1.60*	*0.13 ± 0.05*	*4.89 ± 0.94*	*4.67 ± 0.68*	*1.63 ± 0.47*	*0.07 ± 0.04*	*100.31 ± 2.23*	*15*	*nd*
LTT-25	78.10 ± 0.39	13.54 ± 0.16	0.09 ± 0.01	1.40 ± 0.07	0.18 ± 0.02	0.08 ± 0.02	0.98 ± 0.05	2.61 ± 0.37	2.92 ± 0.40	0.11 ± 0.01	94.31 ± 0.89	15	1
LTT-26	57.23 ± 0.83	14.10 ± 0.78	1.95 ± 0.28	11.54 ± 1.19	3.93 ± 0.70	0.23 ± 0.03	7.31 ± 0.73	2.71 ± 1.11	0.91 ± 0.28	0.10 ± 0.02	100.48 ± 0.46	9	3
Chaitén 2008[1]	75.98 ± 0.45	14.05 ± 0.26	0.12 ± 0.02	1.27 ± 0.11	0.26 ± 0.04	0.06 ± 0.02	1.26 ± 0.13	3.86 ± 0.24	3.14 ± 0.20	nd	98.50 ± 1.62	250	1
VG-568	76.96 ± 0.46	12.18 ± 0.10	0.07 ± 0.01	1.08 ± 0.07	0.03 ± 0.01	0.02 ± 0.02	0.45 ± 0.03	3.52 ± 0.21	4.93 ± 0.04	nd	99.24 ± 0.55	213	
ATHO-G	75.61 ± 0.42	12.20 ± 0.10	0.24 ± 0.02	3.29 ± 0.11	0.10 ± 0.01	0.10 ± 0.02	1.70 ± 0.07	3.75 ± 0.16	2.64 ± 0.05	0.04 ± 0.01	99.63 ± 0.52	192	

	Chaitén 2008[1]	LTT-1	LTT-2	LTT-4	LTT-5	LTT-6
SiO_2	75.98 ± 0.45	76.00 ± 0.51	75.99 ± 0.57	75.54 ± 0.38	76.02 ± 0.52	76.50 ± 0.71
Al_2O_3	14.05 ± 0.26	14.02 ± 0.23	13.98 ± 0.18	13.91 ± 0.15	13.95 ± 0.17	13.56 ± 0.41
TiO_2	0.12 ± 0.02	0.12 ± 0.03	0.12 ± 0.02	0.13 ± 0.01	0.11 ± 0.03	0.10 ± 0.03
FeO	1.27 ± 0.11	1.34 ± 0.14	1.32 ± 0.16	1.30 ± 0.14	1.33 ± 0.12	1.13 ± 0.13
MgO	0.26 ± 0.04	0.22 ± 0.04	0.21 ± 0.05	0.26 ± 0.08	0.18 ± 0.09	0.18 ± 0.05
MnO	0.06 ± 0.02	0.02 ± 0.03	0.03 ± 0.03	0.05 ± 0.02	0.08 ± 0.10	0.06 ± 0.02
CaO	1.26 ± 0.13	1.39 ± 0.13	1.38 ± 0.11	1.42 ± 0.17	1.35 ± 0.08	1.13 ± 0.25
Na_2O	3.86 ± 0.24	3.74 ± 0.47	3.82 ± 0.56	4.46 ± 0.29	3.79 ± 0.48	4.16 ± 0.28
K_2O	3.14 ± 0.20	3.12 ± 0.16	3.11 ± 0.18	2.93 ± 0.19	3.16 ± 0.17	3.14 ± 0.24
Total	98.50 ± 1.62	100.59 ± 0.66	100.66 ± 0.89	100.26 ± 0.67	99.90 ± 1.99	99.95 ± 0.89
n	250	70	102	18	138	37

	LLT-12	LLT-17	LTT-22	LLT-23	LTT-25
SiO_2	76.10 ± 0.21	76.92 ± 0.21	77.09 ± 0.22	77.29 ± 0.34	78.10 ± 0.39
Al_2O_3	14.02 ± 0.12	13.60 ± 0.12	13.35± 0.16	12.97 ± 0.16	13.54 ± 0.16
TiO_2	0.11 ± 0.02	0.08 ± 0.01	0.09 ± 0.01	0.08 ± 0.01	0.09 ± 0.01
FeO	1.23 ± 0.06	1.13 ± 0.05	1.20 ± 0.09	1.15 ± 0.14	1.40 ± 0.07
MgO	0.25 ± 0.03	0.18 ± 0.02	0.17 ± 0.02	0.11 ± 0.03	0.18 ± 0.02
MnO	0.06 ± 0.02	0.06 ± 0.02	0.07 ± 0.03	0.07 ± 0.02	0.08 ± 0.02
CaO	1.20 ± 0.09	0.96 ± 0.04	0.87 ± 0.07	0.80 ± 0.08	0.98 ± 0.05
Na_2O	3.92 ± 0.10	3.77 ± 0.12	3.78 ± 0.09	4.10 ± 0.13	2.61 ± 0.37
K_2O	3.12 ± 0.08	3.31 ± 0.07	3.38 ± 0.08	3.35 ± 0.11	2.92 ± 0.40
Total	97.17 ± 1.82	96.89 ± 2.57	98.99 ± 1.10	101.67 ± 0.50	94.31 ± 0.89
n	48	62	31	16	15